Dynamic Light Scattering Studies of Polymer Solutions. 2. Translational Diffusion and Intramolecular Motions of Polystyrene in Dilute Solutions at the Θ Temperature†

Yoshisuke Tsunashima, Norio Nemoto, and Michio Kurata*

Institute for Chemical Research, Kyoto University, Uji, Kyoto-fu 611, Japan.
Received November 3, 1982

ABSTRACT: Polymer chain dynamics in dilute solution at the Θ temperature has been investigated in the intermediate q region by means of homodyne photon correlation spectroscopy. Narrow molecular weight distribution polystyrenes in *trans*-decahydronaphthalene at 20.4 °C were used for this purpose. The translational diffusion coefficient, the longest intramolecular relaxation time, the relative intensity of the translational diffusive motion, and the effective decay rate have been determined by the bimodal histogram analysis of the measured autocorrelation function. The molecular characteristics have been obtained by extrapolation of these histogram parameters to infinite dilution and/or to zero scattering angle. It has been found that the intramolecular motions of a flexible chain in dilute solution at the Θ temperature can be apparently described in terms of normal mode type motions of the nondraining chain model with preaveraged hydrodynamic interactions. Despite this success, the translational diffusion coefficient, the effective decay rate, and the molecular-weight dependence of the concentration-dependent factor of translational diffusion coefficients are about 15% lower than the theoretical values.

Introduction

Recent development of the dynamic light scattering technique[1] has offered a highly accurate method for studying the dynamic properties of flexible macromolecules in dilute solution over a wide range of X ($=q^2R_G^2$, with q the scattering vector and R_G^2 the mean-square radius of gyration). For $X \ll 1$ or $q^{-1} \gg R_G$ this method gives a direct estimate of the translational diffusion coefficient D, and for smaller q^{-1} as defined by $l \ll q^{-1} \ll R_G$ (l is the statistical segment length) it gives information on the intramolecular relaxation motions in addition to information about the translational motion, both of which are utilized for testing molecular theories of polymer chain dynamics in dilute solution. The test can be made under the Θ condition without being disturbed from the excluded volume effects on the polymer chains.

In a previous paper,[2] we confirmed that histogram analysis is powerful for separate estimation of intramolecular motions and translational diffusive motion.

In this paper, we have studied the polymer chain dynamics at the Θ temperature over a range of X from 0.02 to 10.6 by using a series of high-molecular-weight polystyrenes (PS) in *trans*-decahydronaphthalene (tD) at 20.4 °C. The histogram method has been used for the analysis of the intensity autocorrelation function $A(\tau)$. We have estimated with high reliance the translational diffusion coefficient at infinite dilution D_0, the longest intramolecular relaxation time τ_1, the effective decay rate Γ_e, which is identical with the first cumulant Ω, and the fractional amplitude of the translational diffusive motion a_l, as well as the coefficient k_D of the concentration dependence of D. These characteristics have been used to test the molecular dynamical theories for unperturbed polymer chains at the Θ temperature.

Evaluation of Dynamic Characteristics

The histogram analysis of $A(\tau)$ proceeded according to the procedure described before.[2,3] This procedure, if applied to the data obtained in the intermediate q region, furnishes bimodal distributions of the decay rate Γ, which consists of the first (or slow decay) mode, $l = 1$, representing the translational diffusive motion, and the second (or fast decay) mode, $l = 2$, representing the intramolecular motions. The mean decay rate $\bar{\Gamma}_l$, the amplitude a_l of each mode, and the effective decay rate Γ_e of the whole histogram are related to the dynamic characteristics as

$$\bar{\Gamma}_1/q^2 = D = D_0(1 + k_D c + ...) \quad (1)$$

$$\bar{\Gamma}_2 - \bar{\Gamma}_1 = 2/\tau_c \quad (2)$$

$$\lim_{X,c\to 0} \tau_c = \tau_1 \quad (3)$$

$$a_1 = P_0(X)/P(X) \quad (4)$$

$$\Gamma_e = a_1\bar{\Gamma}_1 + a_2\bar{\Gamma}_2 = \Omega = 1/T^* \quad (5)$$

respectively. Here, c is the polymer concentration in g/cm^3, τ_c is the collective intramolecular relaxation time, which includes contributions from higher relaxation modes than τ_1, and $P_0(X)$ and $P(X)$ are the structure factors for the translational and the total motions at $c \to 0$, respectively. Ω and T^* are the first cumulant[4] and the mean relaxation time,[5] respectively, introduced by other workers.

Table I
Characteristics for PS in *trans*-Decahydronaphthalene at 20.4 °C

sample code	M_w, 10^6	$R_{G,\Theta}^2$, 10^{-11} cm^2	$[\eta]_\Theta$, cm^3/g
FF36	9.70	7.85	240
FF35	5.53	4.56	183
FF33	2.42	1.90	123
F80	0.775	0.609	70.9

Experimental Section

Materials. Four samples of anionically prepared PS in the molecular weight range $M_w = 7.75 \times 10^5$ to 9.70×10^6 with $M_w/M_n \leq 1.04$ (Toyo Soda, Tokyo) were used. Their characteristics in tD at the Θ temperature (20.4 °C)[6] are summarized in Table I. $R_{G,\Theta}$ and $[\eta]_\Theta$ for F80, the sample with the lowest molecular weight, were estimated by using the R_G–M_w and $[\eta]$–M_w relationships.[6] The solvent was prepared by passing the guaranteed reagent grade tD (Tokyo Kasei, Tokyo) through a column of silica gel and then distilling it over sodium metal under an argon atmosphere just prior to use. The boiling temperature was 70.0–71.3 °C at 20 mmHg, and the purity was above 99% as determined by analytical gas chromatography. The density was 0.8695 g/cm^3, the refractive index for 488 nm was 1.4751, and the viscosity was 2.113×10^{-2} g/(cm s) at 20.4 °C.

† An account of this paper was presented at the 30th Polymer Symposium of Japan, Tokyo, Oct 1981.

0024-9297/83/2216-1184$01.50/0

Table II
Results of DLS Measurements for FF36 in *trans*-Decahydronaphthalene at 20.4 °C

	$\bar{\Gamma}_1/\sin^2(\theta/2)/s^{-1}$				
angle, deg	c_1[a]	c_2	c_3	c_4	$c \to 0$
10	1896 ± 29	1928 ± 43	1989 ± 31	2060 ± 21	2112
30	1910 ± 33	1906 ± 49	1986 ± 20	2053 ± 24	2095
60	1901 ± 18	1936 ± 10	1978 ± 1	2049 ± 48	2092
90	1910 ± 27	1921 ± 14	1990 ± 25	2058 ± 49	2102
120	1912 ± 35	1921 ± 6	1990 ± 1	2076 ± 15	2120
150	1908 ± 63	1955 ± 12	1987 ± 6	2049 ± 8	2093
$\theta \to 0$	1906 ± 34	1928 ± 17	1987 ± 17	2058 ± 28	2103 ± 24
	$\bar{\Gamma}_2 - \bar{\Gamma}_1/s^{-1}$				
angle, deg	c_1	c_2	c_3	c_4	$c \to 0$
10	-	-	-	-	-
30	938 ± 69	1011 ± 24	1118 ± 29	1131 ± 81	1226 ± 50
60	1190 ± 117	1161 ± 43	1308 ± 82	1431 ± 95	1497
90	1906 ± 312	1855 ± 230	2020 ± 34	2067 ± 73	2128
120	2998 ± 217	2858 ± 75	2912 ± 139	3107 ± 51	3067
150	3860 ± 146	3799 ± 97	3817 ± 97	3902 ± 19	3882
		$P_0/P \times 10^2$			
angle, deg	X	c_1	c_2	c_3	c_4	$c \to 0$
10	0.0860	100	100	100	100	100
30	0.759	98.1 ± 0.1	98.1 ± 0.6	98.1 ± 0.3	98.5 ± 0.2	98.2 ± 0.3
60	2.831	85.0 ± 0.4	84.4 ± 0.9	85.7 ± 1.6	84.5 ± 2.7	84.9 ± 1.2
90	5.662	62.8 ± 4.6	61.0 ± 2.7	62.1 ± 4.6	61.5 ± 5.2	61.9 ± 4.2
120	8.494	47.1 ± 4.6	44.9 ± 2.5	46.0 ± 3.0	47.4 ± 1.6	46.4 ± 2.9
150	10.566	38.8 ± 2.3	38.6 ± 1.7	38.4 ± 2.4	38.3 ± 3.0	38.5 ± 2.4

[a] Polymer concentration: c_1, 8.44; c_2, 6.28; c_3, 4.40; c_4, 2.22 × 10^{-4} g·cm^{-3}.

Table III
Results of DLS Measurements for Polystyrene in *trans*-Decahydronaphthalene at 20.4 °C

sample code	$(\bar{\Gamma}_1/\sin^2(\theta/2))_{c,\theta\to 0}$, s^{-1}	D_0, 10^{-8} cm^2/s	$D_0 M_w^{1/2}$, 10^{-5} cm^2/s	ρ
FF36	2103 ± 24	1.458	4.54	1.269
FF35	2791 ± 36	1.935	4.55	1.284
FF33	4379 ± 24	3.035	4.72	1.300
F80	7535 ± 17	5.223	4.60	1.267

		k_D(calcd)			
sample code	k_D, cm^3/g	Y-I	P-F	$(\bar{\Gamma}_2 - \bar{\Gamma}_1)_{c,\theta\to 0}$, s^{-1}	A_1
FF36	−119 ± 19	−89.5	−198	1226 ± 50	1.235 ± 0.050
FF35	−104 ± 11	−67.5	−149	2638 ± 46	1.156 ± 0.020
FF33	−82.2 ± 7.3	−40.4	−88.7	9419 ± 267	1.213 ± 0.034
F80	−38.8 ± 2.4	−25.2	−54.8		

Dynamic Light Scattering Measurements. The instrument used was described elsewhere.[7] $A(\tau)$ was measured at 20.4 °C by the time interval method (512 channels) using vertically polarized light of 488 nm, which was emitted from an argon ion laser (Coherent Radiation CR-6) equipped with an oven-stabilized etalon. The vertical component of the scattered light was measured at six scattering angles, 10°, 30°, 60°, 90°, 120°, and 150°. The base line of $A(\tau)$ was located at 1.000 ● 0.002. Dust-free solutions with a variety of concentrations were prepared in a clean cell by mixing by weight the solvent and a solution of appropriate concentration, both of which were centrifuged beforehand. A 12-mm-o.d. NMR tube, free from rack, was used as the light scattering cell. The cell was dipped in a xylene bath in which the temperature was controlled at 20.40 ± 0.02 °C.

Results

We show in Table II the concentration (c) and scattering angle (θ) dependences of $\bar{\Gamma}_1/\sin^2(\theta/2)$, $\bar{\Gamma}_2 - \bar{\Gamma}_1$, and $P_0(X)/P(X)$ for FF36 as a typical example. The corresponding tables of other samples are available on request. The quantity $\bar{\Gamma}_1/\sin^2(\theta/2)$ was practically a constant at each given c, and extrapolation to zero angle was performed to give $(\bar{\Gamma}_1/\sin^2(\theta/2))_{\theta\to 0}$, within 2% deviation, as shown in Table II. At a given θ, $\bar{\Gamma}_1/\sin^2(\theta/2)$ decreased with increasing c, and the linear least-squares extrapolation to infinite dilution gave $(\bar{\Gamma}_1/\sin^2(\theta/2))_{c\to 0}$, shown in the last column of Table II. Then the double extrapolation to $c \to 0$ and $\theta \to 0$ gave $(\bar{\Gamma}_1/\sin^2(\theta/2))_{c,\theta\to 0} = 2103 \pm 24$. k_D was estimated from the concentration dependence of $(\bar{\Gamma}_1/\sin^2(\theta/2))_{\theta\to 0}$.

$\bar{\Gamma}_2 - \bar{\Gamma}_1$ were evaluated to within 5% deviation. At a given θ, the concentration dependence was negative, and the linear least-squares fitting yielded $(\bar{\Gamma}_2 - \bar{\Gamma}_1)_{c\to 0}$ at infinite dilution. Values at smaller scattering angles ($X \ll 1$) were used to evaluate the limiting value $(\bar{\Gamma}_2 - \bar{\Gamma}_1)_{c,\theta\to 0}$. The value can be compared with the theoretical τ_1.

$P_0(X)/P(X)$ were evaluated to within 6% deviation. They showed no concentration dependence for any θ. $(P_0(X)/P(X))_{c\to 0}$ was thus obtained as an average value over four concentrations. The limiting characteristics D_0, k_D, and $(\bar{\Gamma}_2 - \bar{\Gamma}_1)_{c,\theta\to 0}$ for all the polymer samples used are summarized in Table III.

In Table IV, we summarize the c and θ dependences of $\Gamma_e/\sin^2(\theta/2)$ for three samples with higher M_w. At all the θ tested, they showed a negative concentration dependence for each polymer sample, and the linear least-squares fitting gave $(\Gamma_e/\sin^2(\theta/2))_{c\to 0}$ at infinite dilution. The value thus obtained was used to test the X dependence of Ω.

Table IV
Effective Decay Rate for Polystyrenes in *trans*-Decahydronaphthalene at 20.4 °C

angle, deg	X	$\Gamma_e/\sin^2(\theta/2)/s^{-1}$				
		c_1[a]	c_2	c_3	c_4	$c \to 0$
		FF36 ($M_w = 9.70 \times 10^6$)				
10	0.0860	1896 ± 29	1928 ± 43	1989 ± 31	2060 ± 21	2112
30	0.759	2185 ± 82	2257 ± 50	2302 ± 22	2337 ± 33	2400
60	2.831	2770 ± 43	2818 ± 101	2894 ± 63	2956 ± 61	3024
90	5.662	3401 ± 39	3439 ± 17	3476 ± 21	3546 ± 60	3588
120	8.494	3936 ± 81	4017 ± 36	4085 ± 15	4163 ± 47	4245
150	10.566	4390 ± 47	4420 ± 5	4487 ± 36	4532 ± 37	4585
		FF35 ($M_w = 5.53 \times 10^6$)				
10	0.0498	2423 ± 11	2500 ± 17	2557 ± 4	2624 ± 2	2747
30	0.439	2640 ± 26	2704 ± 27	2746 ± 56	2827 ± 31	2932
60	1.637	3152 ± 64	3254 ± 48	3306 ± 42	3377 ± 12	3518
90	3.275	3567 ± 9	3706 ± 5	3737 ± 90	3829 ± 43	3991
120	4.912	4151 ± 8	4220 ± 11	4290 ± 8	4367 ± 26	4496
150	6.111	4460 ± 28	4534 ± 37	4573 ± 21	4649 ± 24	4758
		FF33 ($M_w = 2.42 \times 10^6$)				
10	0.0208	4045 ± 67	4149 ± 11	4230 ± 53	4292 ± 29	4385
30	0.1836	4078 ± 6	4163 ± 42	4232 ± 37	4308 ± 18	4385
60	0.6853	4524 ± 48	4600 ± 60	4699 ± 30	4742 ± 41	4829
90	1.371	4957 ± 92	5051 ± 27	5136 ± 60	5215 ± 13	5305
120	2.056	5312 ± 20	5375 ± 13	5476 ± 48	5572 ± 56	5654
150	2.557	5548 ± 37	5624 ± 9	5713 ± 74	5818 ± 87	5901

[a] Polymer concentration: c_1, 8.44; c_2, 6.28; c_3, 4.40; c_4, 2.22 × 10^{-4} g/cm³ for FF36; c_1, 12.7; c_2, 9.19; c_3, 7.60; c_4, 4.80 × 10^{-4} g/cm³ for FF35; c_1, 8.50; c_2, 6.33; c_3, 4.27; c_4, 2.12 × 10^{-4} g/cm³ for FF33.

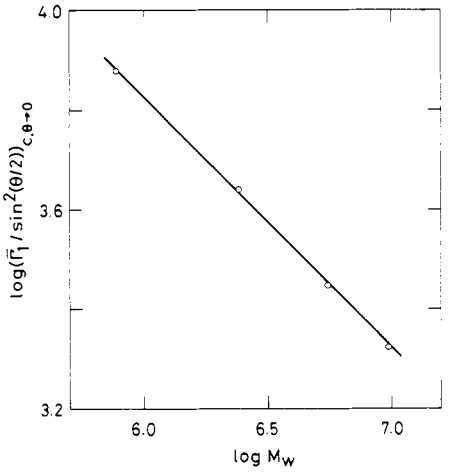

Figure 1. Logarithmic plot of the translational decay rate $(\bar{\Gamma}_1/\sin^2(\theta/2))_{c,\theta\to 0}$, which is proportional to the diffusion coefficient D_0, against molecular weight M_w for polystyrene (PS) in *trans*-decahydronaphthalene (tD) at 20.4 °C. The slope is −0.50.

Discussion

Translational Diffusion Coefficient and Hydrodynamic Radius. The logarithmic plot of $(\bar{\Gamma}_1/\sin^2(\theta/2))_{c,\theta\to 0}$ against M_w is shown in Figure 1. It gives a slope of −0.50 as it should at the Θ temperature. Converting it into D_0 with use of eq 1, we obtain a constant value of $D_0 M_w^{1/2} = (4.60 \pm 0.08) \times 10^{-5}$ cm²/s (Table III).

Recently, Schmidt and Burchard[8] summarized experimental data of D_0 in the molecular weight range $1 \times 10^5 < M_w < 2 \times 10^7$ in terms of a dimensionless number that is defined as the ratio of R_G to the hydrodynamic radius R_H; i.e.

$$\rho = R_G/R_H \tag{6}$$

and

$$R_H = k_B T/6\pi\eta_0 D_0 \tag{7}$$

They have shown that the experimental value, ρ(exptl) = 1.27 ± 0.06, is about 15% smaller than the theoretical ones for monodisperse flexible-chain polymers at the Θ temperature: 1.504 (Kirkwood–Riseman[9] and Benmouna–Akcasu[10]) and 1.479 (Zimm[11]) with the preaveraged Oseen tensor. Our D_0 value leads to ρ(exptl) = 1.28 ± 0.02 (Table III) and confirms the result obtained by Schmidt and Burchard.

Concentration Dependence of the Translational Diffusion Coefficient k_D. At the Θ temperature, k_D is expressed theoretically as

$$k_D = -(N_A/M)(Bv_H + v_1) \tag{8}$$

with $B = 1$ for the Yamakawa–Imai (Y–I) theory[12,13] and $B = 2.23$ for the Pyun–Fixman (P–F) theory of soft interpenetrable spheres with uniform density.[14] Here, v_H is the hydrodynamic volume of the polymer molecule and $v_1 N_A/M$ is the partial specific volume of the polymer, with v_1 the polymer molecular volume, N_A the Avogadro number, and M the molecular weight. If we take a relation that $v_H = (4\pi/3)R_H^3$ with the Stokes law expression, eq 7, and the polymer density 0.910 g/cm³, we can evaluate k_D(calcd) for both theories as

$$k_D(\text{calcd}) = -B' \times 10^{-2} M_w^{1/2} - 1.1 \tag{9}$$

with $B' = 2.73$ (Y–I) and 6.09 (P–F). Here, the experimental result, $D_0 = 4.60 \times 10^{-5} M_w^{-1/2}$, has been used for D_0. The results are listed in Table III. The experimental k_D falls roughly in the middle of two k_D(calcd) values thus estimated.

In a dynamic light scattering study of PS in cyclohexane at 35 °C, King et al.[15] reported a weaker M_w dependence of k_D ($\propto M_w^{0.48}$) in the range $2.1 \times 10^4 \le M_w \le 2.7 \times 10^6$, though the data scattered as shown later. On the other hand, Han[16] and Chu et al.[17] have found that the P–F theory with B independent of M is valid for the PS–cyclohexane system where M_w ranges from 1.30×10^4 to 4.1×10^6. In Figure 2, our experimental k_D data are plotted against M_w, together with other data[15,16] described above. The two solid curves represent k_D(calcd) evaluated from eq 9. The P–F theory is adequate in the lower M_w region,

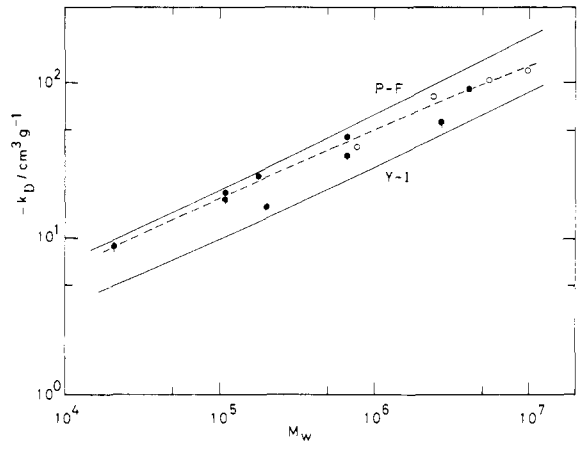

Figure 2. Coefficient k_D for the concentration dependence of the translational diffusion coefficient D plotted against M_w for linear narrow molecular weight distribution PS in Θ solvents with different data sources: (○) present work in tD at 20.4 °C; (●) ref 16 in cyclohexane at 35 °C; (◐) ref 15 in cyclohexane at 35 °C.

but not in the higher M_w region. We thus conclude that neither the P–F nor Y–I theory can describe k_D at the Θ temperature over the entire range of M_w. The present data seem to support the proportionality $k_D \propto M_w^{0.43}$, which is represented by the broken line in the figure. Recent reports[18] also are unable to explain a k_D–M relationship of this form. The molecular weight dependence of $BN_A\upsilon_H/M$ or a revised treatment of υ_H seems to be required.

Longest Internal Relaxation Time τ_1. We define a dimensionless coefficient A_1, which is related to the first eigenvalue λ_1 of the Zimm diffusion equation in polymer chain dynamics:[11]

$$A_1 = M\eta_0[\eta]/\tau_1 RT = M\eta_0[\eta](\bar{\Gamma}_2 - \bar{\Gamma}_1)_{c,\theta\to 0}/2RT \quad (10)$$

where R is the gas constant. The coefficient A_1 depends strongly on the hydrodynamic interaction of the polymer chains. The Rouse theory for free-draining chains leads to $A_1 = 0.822$.[19] For nondraining chains, the Zimm theory gives $A_1 = 1.184$ with the preaveraged Oseen tensor[11] and the Bixon–Zwanzig (B–Z) theory gives $A_1 = 0.574$ without the preaveraged Oseen tensor.[20] We can evaluate A_1 from experimental values of $(\bar{\Gamma}_2 - \bar{\Gamma}_1)_{c,\theta\to 0}$ and $[\eta]$. The results are listed in Table III. They reproduce completely Zimm's value irrespective of M_w (for F80, A_1 may be unreliable because the scattered intensity of the internal motions is too low). There have been reported in the literature a variety of A_1 data, for example, data close to the B–Z value,[21] the Zimm value,[2,22,23] twice the Zimm value,[24] and the Rouse value.[25] The present A_1 data are consistent with our previous data[2] and with the 1979 data of Jones and Caroline.[23]

Relative Intensity of Translational Motion. $(P_0/P(X))_{c\to 0}$ is plotted against X in Figure 3. It produces a universal sigmoidal curve. In the range $X < 6$, the curve agrees well with the theoretical line b $(h' = 2.67)$[2] for the Zimm nondraining chains. This means that the amplitude of normal mode motions can fully be represented by the nondraining chain model. In the region $X > 6$, however, the curve deviates upward and exceeds the line a ($h = 0$ or $h' = 0$) for the Rouse free-draining chains.[26] Here, h' and h denote the hydrodynamic interaction parameters for chains with the number of segments $N = 100$[27] and infinity,[26] respectively.

For the data of FF36 at $\theta = 120°$ and 150°, which correspond to two data points located at about $X = 8.5$ and 10.6 in Figure 3, the bimodal histogram analysis indicated

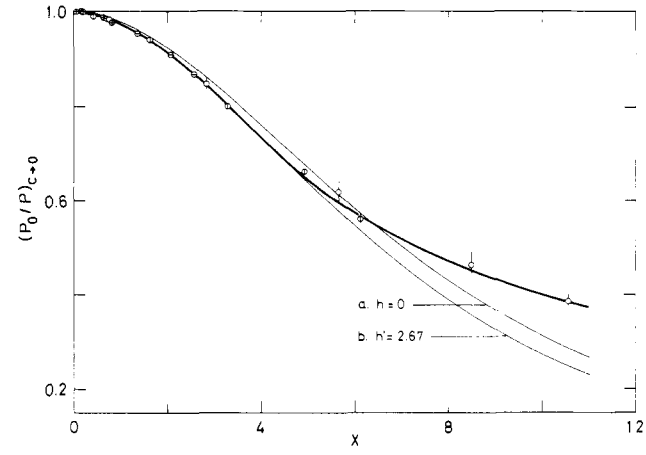

Figure 3. Relative intensity of the translational motion, $(P_0(X)/P(X))_{c\to 0}$, plotted against X for four samples: (○) FF36; (⊕) FF35; (⊖) FF33; (⊕) F80. The vertical bars on the data points denote fitting uncertainties in the histogram analysis. Line a represents the theoretical curve for a free-draining chain ($h = 0$, number of segments $N \to \infty$)[26] and line b the curve for a nondraining chain ($h' = 2.67$, $N = 100$).[2,27]

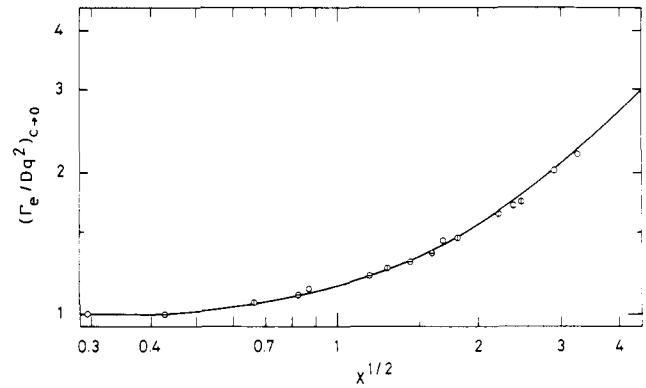

Figure 4. Normalized effective decay rate $(\Gamma_e/Dq^2)_{c\to 0}$ plotted against $X^{1/2}$ for three samples: (○) FF36; (⊕) FF35; (⊖) FF33. The solid curves represents the theoretical curve at the Θ temperature,[10] which is obtained for the nondraining flexible coil with the preaveraged Oseen tensor.

that the Γ distribution for the second (internal) mode became very close to that for the first (translational) mode. Theoretically,[2,27] at $X = 8$, the residual internal intensity term $P - P_0 - P_2$, where P_2 corresponds to the first internal mode, amounts to 29% of the total intensity P and is comparable with P_0 of 39%. At higher X, the residual term increases more. Thus, it is not certain whether the quantity $(P_0/P)_{c\to 0}$ for $X > 8$ can be regarded as a precise measure of the relative amplitude of the translational motion or not.

The result obtained in this section is thus consistent with the result obtained for A_1. The magnitude of relaxation times and of amplitudes of intramolecular motions can be completely represented by normal mode type motions of the nondraining chain with preaveraged hydrodynamic interaction.

Effective Decay Rate Γ_e. The theories at the Θ temperature tell us that in the limit $X \to 0$, Γ_e reduces to D_0q^2 in the Kirkwood approximation, and when $X \to \infty$, it yields a constant value of $\Gamma_e/(k_BT/\eta_0)q^3 = 1/6\pi$[10] for a chain with the preaveraged Oseen tensor and a larger value of $1/16$[28,29] for a chain without the preaveraged Oseen tensor. Our experimental $(\Gamma_e)_{c\to 0}$ corresponding to these two limiting cases mentioned above gives values about 15% smaller than the theoretical ones obtained with the preaveraged Oseen tensor. This result indicates that the theories may

overestimate the magnitude of the decay rates of the internal motions. Experimentally the normalized data $(\Gamma_e/\bar{\Gamma}_1)_{c\to 0}$ may become very close to the theoretical Ω/D_0q^2 values, because our D_0 $(=(\bar{\Gamma}_1)_{c\to 0}/q^2)$ and $(\Gamma_e)_{c\to 0}$ indicate the same magnitude (15%) of deviations from theories.

In Figure 4 we plot the normalized experimental values of $(\Gamma_e/Dq^2)_{c\to 0}$ against $X^{1/2}$ for three samples with higher M_w. The solid curve represents the theoretical curve[4,10] calculated for the nondraining flexible coil with the preaveraged Oseen tensor at the Θ temperature. All the data points fall completely on the theoretical curve. It should be noted that the theoretical curve calculated without the preaveraged Oseen tensor results in a worse fit. As far as we see the normalized quantity Γ_e/D_0q^2, we thus confirm the validity of the nondraining chain model with the preaveraged hydrodynamic interaction.

A similar result has been obtained by Han and Akcasu.[30] They have studied the X dependence of the first cumulant Ω divided by q^3k_BT/η_0 on PS in cyclohexane at 35 °C and found that the data agree, with the same magnitude of deviation as ours, with the theoretical predictions with the preaveraged Oseen tensor. In the range $X^{1/2} > 2$, they have estimated Ω by shape function analysis. As mentioned before, Ω and Γ_e are identical in definition but are estimated by different analytical methods. In order to test this identity, we have analyzed our $A(\tau)$ data by using the asymptotic shape function in parallel with the histogram method. The results indicate that Ω gives a value only 3–6% larger than Γ_e within the limit of experimental error when $X^{1/2} > 2$. The difference does not alter the conclusion described above.[31]

In conclusion, we can affirm that the dynamic behavior of a polymer chain in dilute solution at the Θ temperature is apparently described by the nondraining chain model with preaveraged hydrodynamic interaction. A 15% difference between theories and experiments observed in D_0, in $(\Gamma_e)_{c\to 0}$, and also in the exponent of M_w dependence of k_D indicates that serious defects are involved in the present theories especially in the treatment of hydrodynamic interactions of polymer chains in dilute solution.

Registry No. Polystyrene, 9003-53-6.

References and Notes

(1) Berne, B. J.; Pecora, R. "Dynamic Light Scattering"; Wiley: New York, 1976.
(2) Tsunashima, Y.; Nemoto, N.; Kurata, M. *Macromolecules* **1983**, *16*, 584.
(3) (a) Tsunashima, Y.; Nemoto, N.; Makita, Y.; Kurata, M. *Bull. Inst. Chem. Res., Kyoto Univ.* **1980**, *59*, 293. (b) Gulari, E.; Gulari, E.; Tsunashima, Y.; Chu, B. *J. Chem. Phys.* **1979**, *70*, 3965.
(4) Akcasu, A. Z.; Benmouna, M.; Han, C. C. *Polymer* **1980**, *21*, 866.
(5) (a) Buldt, G. *Macromolecules* **1976**, *9*, 606. (b) Freire, J. J. *Polymer* **1978**, *19*, 1441.
(6) Fukuda, M.; Fukumoto, M.; Kato, Y.; Hashimoto, T. *J. Polym. Sci., Polym. Phys. Ed.* **1974**, *12*, 871.
(7) Nemoto, N.; Tsunashima, Y.; Kurata, M. *Polym. J.* **1981**, *13*, 827.
(8) Schmidt, M.; Burchard, W. *Macromolecules* **1981**, *14*, 210.
(9) Kirkwood, J. G.; Riseman, J. *J. Chem. Phys.* **1948**, *16*, 565.
(10) Benmouna, M.; Akcasu, A. Z. *Macromolecules* **1978**, *11*, 1187.
(11) Zimm, B. H. *J. Chem. Phys.* **1956**, *24*, 269.
(12) Yamakawa, H. "Modern Theory of Polymer Solutions"; Harper and Row: New York, 1971; Chapter 6.
(13) Imai, S. *J. Chem. Phys.* **1969**, *50*, 2116.
(14) Pyun, C. W.; Fixman, M. *J. Chem. Phys.* **1964**, *41*, 937.
(15) King, T. A.; Knox, A.; Lee, W. I.; McAdam, J. D. G. *Polymer* **1973**, *14*, 151.
(16) Han, C. C. *Polymer* **1979**, *20*, 259.
(17) Gulari, E.; Gulari, E.; Tsunashima, Y.; Chu, B. *Polymer* **1979**, *20*, 347.
(18) (a) Akcasu, A. Z.; Benmouna, M. *Macromolecules* **1978**, *11*, 1193. (b) Akcasu, A. Z. *Polymer* **1981**, *22*, 1169. (c) Mulderije, J. J. H. *Macromolecules* **1980**, *13*, 1526.
(19) Rouse, P. E. *J. Chem. Phys.* **1953**, *21*, 1272.
(20) Bixon, M.; Zwanzig, R. *J. Chem. Phys.* **1978**, *68*, 1890.
(21) Jones, G.; Caroline, D. *Chem. Phys. Lett.* **1978**, *58*, 149.
(22) Huang, W.; Frederick, J. E. *Macromolecules* **1974**, *7*, 34.
(23) Jones, G.; Caroline, D. *Chem. Phys.* **1979**, *37*, 187.
(24) King, T. A.; Treadaway, M. F. *J. Chem. Soc., Faraday Trans. 2* **1976**, *72*, 1473.
(25) McAdam, J. D. G.; King, T. A. *Chem. Phys. Lett.* **1974**, *28*, 90.
(26) Pecora, R. *J. Chem. Phys.* **1968**, *49*, 1032.
(27) Perico, A.; Piaggio, P.; Cuniberti, C. *J. Chem. Phys.* **1975**, *62*, 2690.
(28) Benmouna, M.; Akcasu, A. Z. *Macromolecules* **1980**, *13*, 409.
(29) Burchard, W.; Schmidt, M.; Stockmayer, W. H. *Macromolecules* **1980**, *13*, 580.
(30) Han, C. C., private communication. Han, C. C.; Akcasu, A. Z. *Macromolecules* **1981**, *14*, 1080.
(31) Tsunashima, Y.; Nemoto, N. *J. Polym. Sci., Polym. Lett. Ed.*, in press.

Molecular Weight Effects of Triplet Sensitization of Poly(4-vinylbiphenyl) in Benzene

James F. Pratte and S. E. Webber*

Department of Chemistry and Center for Polymer Research, The University of Texas at Austin, Austin, Texas 78712.

Received October 27, 1982

ABSTRACT: The rate of sensitization of the triplet state of poly(4-vinylbiphenyl) (P4VBP) is measured for a number of triplet-state donors. The dependence of the sensitization rate (k_Q) on the energy of the triplet-state donor implies at least two acceptor states are present in P4VBP, one at ca. 67 kcal/mol (shifted to slightly lower energy relative to 4-methylbiphenyl) and the other at ca. 56 kcal/mol, which is assigned to a polymer-bound species, probably an end group. It has been found that $k_Q \propto P^{-0.45}$, in good agreement with the exponential value predicted from earlier work. The fluorescence of the P4VBP has demonstrated the presence of at least two species in addition to normal biphenyl. One of these is correlated with the species with a low-energy triplet state, but the other abnormal species is not identified. Because of the molecular weight dependence of these two abnormal species it is likely that they are both end groups.

Introduction

In previous studies on the triplet-state quenching and sensitization of poly(2-vinylnaphthalene) (P2VN) in room-temperature benzene solutions, a molecular weight dependence of the bimolecular rate constant for the small molecule–polymer reaction has been observed.[1,2] As part of our ongoing study of the triplet-state properties of poly(vinyl aromatics), we have investigated the triplet sensitization of poly(4-vinylbiphenyl) (P4VBP). Once again, a molecular weight effect in the bimolecular rate

0024-9297/83/2216-1188$01.50/0